An Acad Bras Cienc (2024) 96(1): e20220875 DOI 10.1590/0001-3765202420220875
Anais da Academia Brasileira de Ciências | *Annals of the Brazilian Academy of Sciences*
Printed ISSN 0001-3765 I Online ISSN 1678-2690
www.scielo.br/aabc | www.fb.com/aabcjournal

CHEMICAL SCIENCES

Development of benzaldehyde-pyrazoline hybrids for functionalization of polymers with fluorescent pendant moieties

GHEORGHE ROMAN, MIHAELA BALAN-PORCĂRAŞU & LIVIU SĂCĂRESCU

Abstract: Compounds with a pyrazoline scaffold are useful as sensors for fluorescence detection of different types of analytes. Recovery of a pyrazoline-based sensor with a view to use it recurrently would be more facile when the sensing molecule is attached to a solid support. A reaction sequence has been designed to synthesize two benzaldehyde–pyrazoline hybrids as examples of a hitherto unknown type of compounds to be employed for the potential derivatization of polymers containing primary amino groups through azomethine formation. All intermediates, including the fairly unstable N^1-unsubstituted pyrazolines, along with the target compounds have been structurally characterized, with an emphasis on their particular NMR features. Examination of the photophysical properties of these benzaldehyde–pyrazoline hybrids showed that, despite the shortening of the extended N1-N2-C3 conjugated system common to 1,3,5-triarylpyrazolines through the replacement of the aryl at N1 by an aryloxyacetyl moiety, the novel compounds exhibit emission maxima at approximately 350 nm. Moreover, the introduction of a moderately electron-withdrawing substituent such as chlorine in the phenyl at C3 of pyrazoline leads to an amplification of fluorescence intensity.

Key words: aromatic aldehyde, luminescence, multistep synthesis, pyrazoline.

INTRODUCTION

In the last decade, the intrinsic fluorescence of pyrazolines has been exploited for the development of chemosensors useful for the detection of various analytes (such as metal cations, including those that have proven harmful to the environment, anions or biotic molecules) in solution and even in living cells (Varghese et al. 2017, Săcărescu et al. 2023, Mahesha et al. 2022). Moreover, selected pyrazolines have been combined with polymeric materials with a view to provide access to novel materials useful for photonic applications (Szukalski et al. 2015), polymer-supported molecular logic gates responsive to acidity and oxidation (Zerafa et al. 2021), or have even been incorporated onto polymer backbone to afford blue fluorescent materials suitable for electroluminescent devices (Liao et al. 2017). Our group has recently developed a pyrazoline having a 4-(benzyloxy)-phenyl substituent at position 5 which was shown to possess fluorescence that is selectively quenched by chloroalkanes (Chibac et al. 2019a), and which also proved to be an efficient testing system for chloride anions (Chibac et al. 2019b). Furthermore, the same pyrazoline was shown to associate in solution with short chains of low molecular weight polysilane to form nano-aggregates whose optical properties could be useful for the development of innovative sensing devices with potential applications in medicine (Chibac-Scutaru et al. 2020). The

current study aims at investigating a synthetic approach towards the functionalization of pyrazolines at N^1 with a benzaldehyde moiety and at examining these compounds' photophysical properties. With a view to further explore the synthesis, optical properties and sensing ability of polymers that incorporate fluorescent pyrazolines in their structure, the target compounds could be subsequently attached as pendant groups through an azomethine function by reacting them with a wide range of polymers containing primary amino groups, *e.g.* natural chitosan (Antony et al. 2019), semi-synthetic amino cellulose (Heinze et al. 2016), or synthetic macromolecules such as poly(ethyleneimine)-containing copolymers (Chen et al. 2020), aminoalkyl functionalized polysiloxanes (Łubkowska & Stańczyk 2014) or aminoalkyl-substituted polysilanes (Mangala & Sreekumar 2015).

MATERIALS AND METHODS

All reagents and solvents were purchased from commercial suppliers (Sigma–Aldrich, TCI Europe N.V., Merck KGaA) and were used without further purification. Melting points were determined on a Mel Temp II apparatus and are uncorrected. Fourier transform-infrared (FTIR) spectra were taken on a Bruker Vertex 70 spectrophotometer in the transmission mode in the wavenumber range of 400 to 4000 cm^{-1} using KBr pellets. NMR spectra were recorded on a Bruker Avance NEO spectrometer operating at 400 MHz, with a 5 mm probe for direct detection of ^{1}H, ^{13}C, ^{19}F and ^{29}Si. The spectra were recorded at room temperature using the standard parameter sets provided by Bruker. The residual signals of the deuterated solvents were used as internal standard (DMSO-d_6: δ = 2.51 ppm for ^{1}H and δ = 39.5 ppm for ^{13}C; $CDCl_3$: δ = 7.26 ppm for ^{1}H and δ = 77.0 ppm for ^{13}C). The assignment of the signals in the ^{1}H and ^{13}C NMR spectra was based on additional 2D homo- and hetero-nuclear correlation experiments (H,H-COSY, H,C-HSQC and H,C-HMBC). For NMR analysis purposes, the numbering of the structures reported in this study is given in Figure S1 in Supplementary Material. Elemental analysis was performed on a Vario EL III CHNS analyzer. Electronic absorption spectra (UV–vis) of compounds **12** and **13** were recorded in tetrahydrofuran (THF), at a concentration of approximately 10^{-5} M, at room temperature. The solutions were placed in standard UV quartz spectrometer cuvette cells with a path length of 1 cm, and the spectra were recorded using a SPECORD 210 Plus Analytik Jena spectrophotometer. Fluorescence spectra of compounds **12** and **13** (C = 10^{-5} M) were recorded with a RF-6000 Shimadzu spectrofluorometer in THF, at room temperature, using as excitation wavelength the absorption maximum identified in the UV–vis spectra of these compounds (λ_{ex} = 292 nm).

Experimental procedures

Synthesis of benzyloxy-substituted chalcone analogs – general procedure

A solution of 4-(benzyloxy)benzaldehyde **1** (2.12 g, 10 mmol) and either acetophenone **2**, or 4-chloroacetophenone **3** or 4-methoxyacetophenone **4** (10 mmol) in 96% ethanol (20 mL) was treated with 40% aq. NaOH (0.2 mL). The reaction mixture was stirred at room temperature for 1 h, and then the resulting suspension of the chalcone analog was set aside overnight. The solid was filtered, washed sequentially with hexanes (2 × 15 mL) and a mixture of hexanes–2-propanol (15 mL, 1:2 *v*/*v*), and air-dried. The material was dissolved in chloroform (25 mL), the resulting light suspension was filtered gravitationally, and then chloroform from the filtrate was removed under

reduced pressure to give the crude chalcone, which was recrystallized from the appropriate solvent.

3-[4-(Benzyloxy)phenyl]-1-phenylprop-2-ene-1-one (5)

Yellowish needles from ethyl acetate or yellowish plates from ethanol, yield 71%, mp 117–118 °C (lit. (Iftikhar et al. 2017) mp 120 °C). ^{1}H NMR ($CDCl_3$, 400 MHz), δ (ppm): 5.12 (s, 2H, H10), 7.02 (d, J = 8.8 Hz, 2H, H6 and H8), 7.31–7.47 (m, 6H, H2, H12–H16), 7.47–7.54 (m, 2H, H19 and H21), 7.54–7.65 (m, 3H, H5, H9 and H20), 7.79 (d, J = 15.6 Hz, 1H, H3), 8.01 (d, J = 8.4 Hz, 2H, H18 and 22). ^{13}C NMR ($CDCl_3$, 100 MHz), δ (ppm): 70.1 (C10), 115.3 (C6 and C8), 119.9 (C2), 127.5 (C12 and C16), 127.9 (C14), 128.2 (C4), 128.4 (C18 and C22), 128.6 (C19 and C21), 128.7 (C13 and C15), 130.2 (C5 and C9), 132.6 (C20), 136.4 (C11), 138.5 (C6), 144.6 (C3), 160.8 (C7), 190.6 (C1).

3-[4-(Benzyloxy)phenyl]-1-(4-chlorophenyl) prop-2-ene-1-one (6)

Colorless needles from ethyl acetate, yield 66%, mp 133–134 °C. ^{1}H NMR ($CDCl_3$, 400 MHz), δ (ppm): 5.15 (s, 2H, H10), 7.04 (d, J = 8.8 Hz, 2H, H6 and H8), 7.34–7.53 (m, 8H, H2, H12–H16, H19 and H21), 7.63 (d, J = 8.8 Hz, 2H, H5 and H9), 7.82 (d, J = 15.6 Hz, 1H, H3), 7.98 (d, J = 8.8 Hz, 2H, H18 and H22). ^{13}C NMR ($CDCl_3$, 100 MHz), δ (ppm): 70.1 (C10), 115.3 (C6 and C8), 119.3 (C2), 127.5 (C12 and C16), 127.7 (C4), 128.2 (C14), 128.7 (C13 and C15), 128.9 (C19 and C21), 129.8 (C18 and C22), 130.3 (C5 and C9), 136.3 (C11), 136.8 (C17), 139.0 (C20), 145.1 (C3), 161.0 (C7), 189.2 (C1).

3-[4-(Benzyloxy)phenyl]-1-(4-methoxyphenyl) prop-2-ene-1-one (7)

Colorless plates from ethyl acetate, yield 57%, mp 117–118 °C (lit. (Bale et al. 2018) mp 135–137 °C). ^{1}H NMR ($CDCl_3$ 400 MHz), δ (ppm): 3.89 (s, 3H, H23), 5.12 (s, 2H, H10), 6.98 (d, J = 8.8 Hz, 2H, H19 and H21), 7.01 (d, J = 8.4 Hz, 2H, H6 and H8), 7.31–7.48 (m, 6H, H2, H12–H16), 7.60 (d, J = 8.8 Hz, 2H, H5 and H9), 7.78 (d, J = 15.6 Hz, 1H, H3), 8.03 (d, J = 8.8 Hz, 2H, H6 and H8). ^{13}C NMR ($CDCl_3$, 100 MHz), δ (ppm): 55.5 (C23), 70.1 (C10), 113.8 (C19 and C21), 115.3 (C6 and C8), 119.7 (C2), 127.5 (C12 and C16), 128.0 (C4), 128.2 (C14), 128.7 (C13 and C15), 130.1 (C5 and C9), 130.7 (C18 and C22), 131.3 (C17), 136.4 (C11), 143.7 (C3), 160.7 (C7), 163.3 (C20), 188.7 (C1).

Synthesis of N1-unsubstituted pyrazolines – general procedure

A suspension of chalcone analog **5**, **6** or **7** (4 mmol) in 2-propanol (20 mL) was treated with hydrazine hydrate (800 mg), and then the mixture was heated at reflux temperature for 4 h. Refrigeration of the reaction mixture overnight afforded a solid, which was filtered, washed with a mixture of hexanes–2-propanol (2 × 10 mL, 1:1 v/v), and then air-dried to give the title compounds.

5-[4-(Benzyloxy)phenyl]-3-phenyl-4,5-dihydro-1H-pyrazole (8)

Colorless crystals, yield 96%, mp 108–109 °C (ethanol). ^{1}H NMR (DMSO-d_6, 400 MHz), δ (ppm): 2.82 (dd, J_{AX} = 10.6 Hz and J_{AM} = 16.2 Hz, 1H, C2-H_A), 3.40 (dd, J_{MX} = 10.6 Hz and J_{AM} = 16.2 Hz, 1H, C2-H_M), 4.79 (td, J_{MX} = J_{AX} = 10.6 Hz and $J_{NH\text{-}Hx}$ = 2.5 Hz, 1H, C3-H_X), 5.10 (s, 2H, H10), 6.99 (d, J = 8.8 Hz, 2H, H6 and H8), 7.29–7.35 (m, 4H, H5, H9, H14 and H20), 7.37–7.41 (m, 4H, H13, H15, H19 and H21), 7.45 (d, J = 7.0 Hz, 2H, H12 and H16), 7.52 (d, J = 3.2 Hz, 1H, NH), 7.63 (d, 7.2 Hz, 2H, H18 and H22). ^{13}C NMR (DMSO-d_6, 100 MHz), δ (ppm): 40.5 (C2), 63.2 (C3), 69.1 (C10), 114.7 (C6 and C8), 125.3 (C18 and C22), 127.6 (C12 and C16), 127.7 (C5, C9 and C14), 128.0 (C20), 128.4 (either C13 and C15, or C19 and C21), 128.5 (either C19 and C21, or C13 and C15), 133.3 (C17), 135.1 (C4), 137.1 (C11), 148.5 (C1), 157.5 (C7).

5-[4-(Benzyloxy)phenyl]-3-(4-chlorophenyl)-4,5-dihydro-1H-pyrazole (9)

Colorless solid, yield 94%, mp 127–128 °C. ^{1}H NMR (DMSO-d_6, 400 MHz), δ (ppm): 2.82 (dd, J_{AX} = 10.7 Hz and J_{AM} = 16.3 Hz, 1H, C2-H_A), 3.39 (dd, J_{MX} = 10.7 Hz and J_{AM} = 16.3 Hz, 1H, C2-H_M), 4.81 (td, J_{MX} = J_{AX} = 10.7 Hz and J_{NH-Hx} = 2.9 Hz, 1H, C3-H_X), 5.10 (s, 2H, H10), 6.99 (d, J = 8.4 Hz, 2H, H6 and H8), 7.28–7.35 (m, 3H, H5, H9 and H14), 7.39 (t, J = 7.3 Hz, 2H, H13 and H15), 7.43–7.46 (m, 4H, H12, H16, H19 and H21), 7.62–7.64 (m, 3H, H18, H22 and NH). ^{13}C NMR (DMSO-d_6, 100 MHz), δ (ppm): 40.2 (C2), 63.3 (C3), 69.1 (C10), 114.7 (C6,8), 126.9 (C18 and C22), 127.6 (C12 and C16), 127.7 (C5, C9 and C14), 128.4 (C13 and C15), 128.5 (C19 and C21), 132.2 (C17), 132.3 (C20), 134.9 (C4), 137.1 (C11), 147.3 (C1), 157.5 (C7).

Synthesis of 1-(bromoacetyl)pyrazolines – general procedure

To an efficiently stirred solution of N^1-unsubstituted pyrazoline **8** or **9** (1.2 mmol) in chloroform (10 mL) were sequentially added anh. K_2CO_3 (414 mg, 3 mmol) and a solution of bromoacetyl bromide (363 mg, 1.8 mmol) in chloroform (5 mL). After the mixture had been stirred at room temperature overnight, the inorganics were removed by filtration, and then the solvent in the filtrate was removed under reduced pressure. The resulting oil, which slowly turned into a crystalline solid when kept on the bench overnight, was recrystallized from the appropriate solvent.

1-{5-[4-(Benzyloxy)phenyl]-3-phenyl-4,5-dihydro-1H-pyrazol-1-yl}-2-bromoethanone (10)

Colorless crystals from 2-propanol, yield 83%, mp 146–147 °C. ^{1}H NMR ($CDCl_3$, 400 MHz), δ (ppm): 3.22 (dd, J_{AX} = 4.5 Hz and J_{AM} = 17.8 Hz, 1H, C2-H_A), 3.76 (dd, J_{MX} = 11.7 Hz and J_{AM} = 17.8 Hz, 1H, C2-H_M), 4.32 (d, J = 10.4 Hz, 1H, H24a), 4.35 (d, J = 10.4 Hz, 1H, H24b), 5.03 (s, 2H, H10), 5.55 (dd, J_{AX} = 4.5 Hz and J_{MX} = 11.7 Hz, 1H, C3-H_X), 6.93 (d, J = 8.8 Hz, 2H, H6 and H8), 7.19 (d, J = 8.8 Hz, 2H, H5 and H9), 7.28–7.50 (m, 8H, H12–H16, H19–H21), 7.77 (dd, J = 2.2 and 8.0 Hz, 2H, H18 and H22). ^{13}C NMR ($CDCl_3$, 100 MHz), δ (ppm): 27.5 (C24), 42.3 (C2), 59.9 (C3), 70.0 (C10), 115.2 (C6 and C8), 126.8 (C18 and C22), 127.0 (C5 and C9), 127.5 (C12 and C16), 128.0 (C14), 128.6 (either C13 and C15, or C19 and C21), 128.8 (either C19 and C21, or C13 and C15), 130.8 (C20), 130.9 (C17), 133.3 (C4), 136.9 (C11), 155.3 (C1), 158.5 (C7), 164.1 (C23).

1-{5-[4-(Benzyloxy)phenyl]-3-(4-chlorophenyl)-4,5-dihydro-1H-pyrazol-1-yl}-2-bromoethanone (11)

Yellowish crystals from 96% ethanol, yield 72%, mp 114–115 °C. ^{1}H NMR ($CDCl_3$, 400 MHz), δ (ppm): 3.18 (dd, J_{AX} = 4.6 Hz and J_{AM} = 17.8 Hz, 1H, C2-H_A), 3.74 (dd, J_{MX} = 11.7 Hz and J_{AM} = 17.8 Hz, 1H, C2-H_M), 4.29 (d, J = 10.4 Hz, 1H, H24a), 4.32 (d, J = 10.4 Hz, 1H, H24b), 5.03 (s, 2H, H10), 5.55 (dd, J_{AX} = 4.6 Hz and J_{MX} = 11.7 Hz, 1H, C3-H_X), 6.93 (d, J = 8.8 Hz, 2H, H6 and H8), 7.17 (d, J = 8.8 Hz, 2H, H5 and H9), 7.29–7.46 (m, 7H, H12–16, H19 and H21), 7.69 (d, J = 8.8 Hz, 2H, H18 and H22). ^{13}C NMR ($CDCl_3$, 100 MHz), δ (ppm): 27.3 (C24), 42.3 (C2), 60.1 (C3), 70.1 (C10), 115.3 (C6 and C8), 127.0 (C5 and C9), 127.5 (C12 and C16), 128.0 (C14), 128.1 (C18 and C22), 128.6 (C19 and C21), 129.1 (C13 and C15), 129.5 (C17), 133.1 (C4), 136.8 (C11), 136.9 (C20), 154.1 (C1), 158.5 (C7), 164.1 (C23).

Synthesis of benzaldehyde–pyrazoline hybrids – general procedure

4-Hydroxybenzaldehyde (97.6 mg, 0.8 mmol) was dissolved in a solution of KOH (53 mg, 0.8 mmol, 85% purity) in 96% ethanol (10 mL). 1-(Bromoacetyl)pyrazoline **10** or **11** (0.8 mmol) was then added in one portion to the solution, and the resulting mixture was heated at reflux temperature for 1 h. The suspension was allowed to reach room temperature, and then it

was gradually diluted with water (40 mL) under efficient stirring. The solid material was filtered, washed thoroughly with water, air-dried, and recrystallized from the appropriate solvent.

4-{2-{5-[4-(Benzyloxy)phenyl]-3-phenyl-4,5-dihydro-1H-pyrazol-1-yl}-2-oxoethoxy} benzaldehyde (12)

Colorless crystals from 96% ethanol, yield 60%, mp 159–160 °C. ^{1}H NMR ($CDCl_3$, 400 MHz), δ (ppm): 3.26 (dd, J_{AX} = 4.4 Hz and J_{AM} = 17.6 Hz, 1H, C2-H_A), 3.78 (dd, J_{MX} = 11.7 Hz and J_{AM} = 17.8 Hz, 1H, C2-H_M), 5.03 (s, 2H, H10), 5.21 (d, J = 16.0 Hz, 1H, H24a), 5.26 (d, J = 16.0 Hz, 1H, H24b), 5.58 (dd, J_{AX} = 4.4 Hz and J_{MX} = 11.6 Hz, 1H, C3-H_X), 6.91 (d, J = 8.8 Hz, 2H, H6 and H8), 7.03 (d, J = 8.8 Hz, 2H, H26 and H30), 7.19 (d, J = 8.4 Hz, 2H, H5 and H9), 7.28–7.43 (m, 5H, H12–H16), 7.43–7.51 (m, 3H, H19–H21), 7.75–7.84 (m, 4H, H18, H22, H27 and H29), 9.87 (s, 1H, H31). ^{13}C NMR ($CDCl_3$, 100 MHz), δ (ppm): 41.8 (C2), 60.0 (C3), 66.1 (C24), 70.1 (C10), 115.1 (C26 and C30), 115.2 (C6 and C8), 126.8 (C18 and C22), 127.2 (C5 and C9), 127.4 (C12 and C16), 128.0 (C14), 128.6 (C13 and C15), 129.0 (C19 and C21), 130.3 (C28), 130.8 (C17), 130.9 (C20), 131.9 (C27 and C29), 133.3 (C4), 136.8 (C11), 155.8 (C1), 158.5 (C7), 163.4 (C25), 164.6 (C23), 190.8 (C31). *Anal.* Calc. for $C_{31}H_{26}N_2O_4$ (490): C, 75.90; H, 5.34; N, 5.71. Found: C, 75.57; H, 5.04; N, 5.49.

4-{2-{5-[4-(Benzyloxy)phenyl]-3-(4-chlorophenyl)-4,5-dihydro-1H-pyrazol-1-yl}-2-oxoethoxy}benzaldehyde (13)

Colorless crystals from 96% ethanol–ethyl acetate (1:1, *v*/*v*), yield 48%, mp 190–191 °C. ^{1}H NMR ($CDCl_3$, 400 MHz), δ (ppm): 3.22 (dd, J_{AX} = 4.7 Hz and J_{AM} = 17.8 Hz, 1H, C2-H_A), 3.75 (dd, J_{MX} = 11.8 Hz and J_{AM} = 17.8 Hz, 1H, C2-H_M), 5.03 (s, 2H, H10), 5.19 (d, J = 16.0 Hz, 1H, H24a), 5.23 (d, J = 16.0 Hz, 1H, H24b), 5.58 (dd, J_{AX} = 4.7 Hz and J_{MX} = 11.8 Hz, 1H, C3-H_X), 6.91 (d, J = 8.4 Hz, 2H, H6 and H8), 7.02 (d, J = 8.8 Hz, 2H, H26 and H30), 7.17 (d, J = 8.4 Hz, 2H, H5 and H9), 7.28–7.47 (m, 7H, H12–H16, H19 and H21), 7.70 (d, J = 8.4 Hz, 2H, H18 and H22), 7.80 (d, J = 8.4 Hz, 2H, H27 and H29), 9.87 (s, 1H, H31). ^{13}C NMR ($CDCl_3$, 100 MHz), δ (ppm): 41.7 (C2), 60.1 (C3), 66.1 (C24), 70.1 (C10), 115.0 (C6 and C8), 115.3 (C26 and C30), 127.2 (C5 and C9), 127.4 (C12 and C16), 128.0 (C18 and C22), 128.6 (C13 and C15), 129.2 (C17, C19 and C21), 129.3 (C14), 130.4 (C28), 131.9 (C27 and C29), 133.1 (C4), 136.8 (C11), 136.9 (C20), 154.6 (C1), 158.6 (C7), 163.3 (C25), 164.6 (C23), 190.8 (C31). *Anal.* Calc. for $C_{31}H_{25}ClN_2O_4$ (524.5): C, 70.92; H, 4.80; N, 5.34. Found: C, 70.63; H, 4.48; N, 5.01.

RESULTS AND DISCUSSION

The main reason for the success story of pyrazolines in materials chemistry can be undeniably traced back to their facile preparation. The preferred synthetic approach to pyrazolines relies on the cyclocondensation of α,β-unsaturated carbonyl compounds (especially chalcone analogs) with hydrazine derivatives (Vahedpour et al. 2021, Farooq & Ngaini 2019, Lévai 2002). This robust synthetic approach allows for a versatile installment of the desired substituents at positions 1, 3 and 5 of pyrazoline through the careful selection of the (hetero)aryl methyl ketone, (hetero) aromatic aldehyde and hydrazine derivative employed as starting materials. Because the presence of a 4-(benzyloxy)phenyl moiety at position 5 of pyrazoline is a requisite in our case, 4-(benzyloxy)-benzaldehyde **1** was chosen as the starting aromatic aldehyde in the synthesis of the target compounds, but the nature of the substituent at position 3 of target pyrazolines was diversified through the use of several starting aryl methyl ketones **2**–**4** (Figure 1). Claisen condensation of these reagents in 96% ethanol in the presence of NaOH afforded the desired chalcone analogs **5**–**7** having a 4-(benzyloxy)phenyl moiety at position 3 of the propenone segment of the molecule. Under the

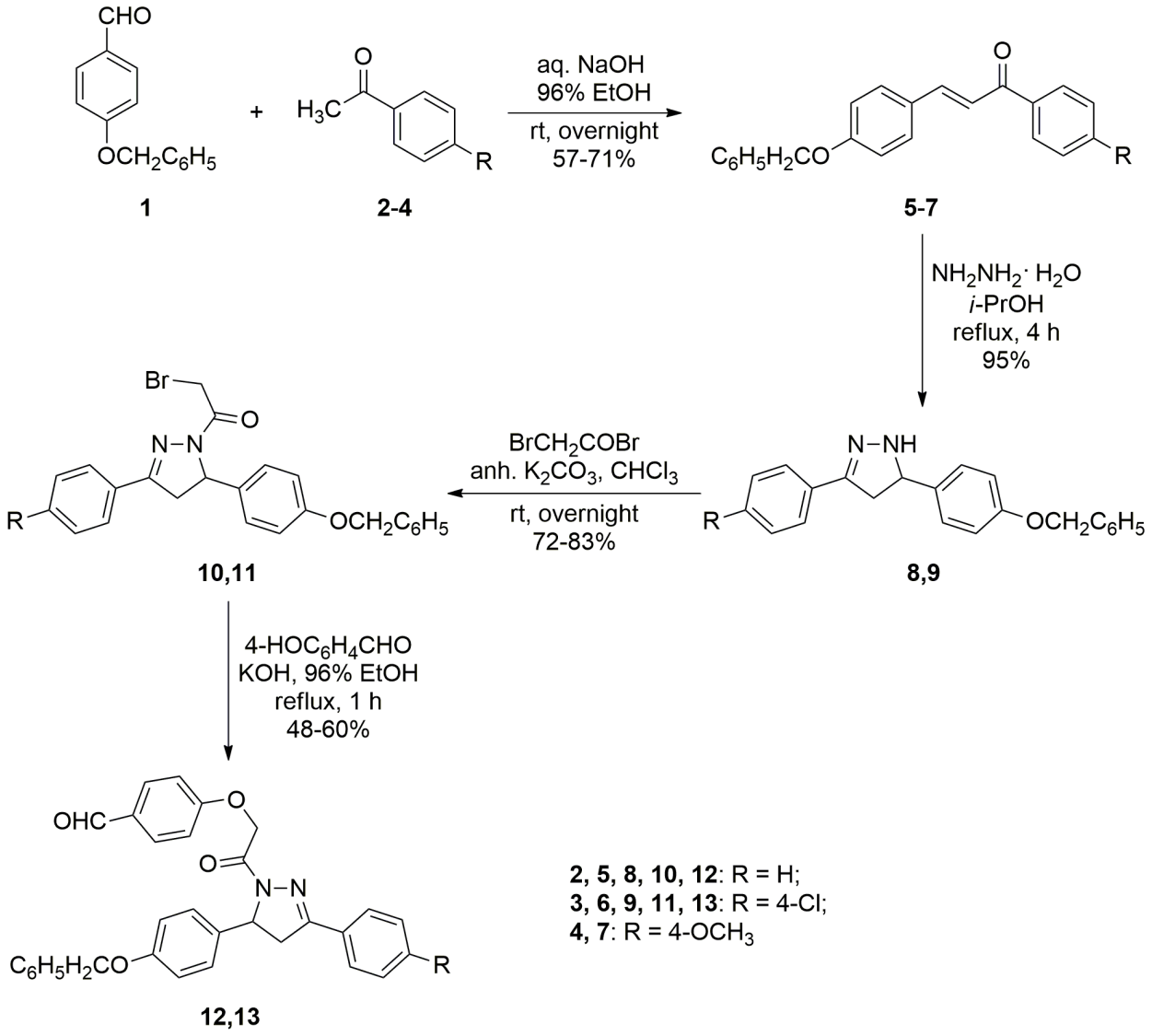

Figure 1. Reaction sequence leading to the target benzaldehyde–pyrazoline hybrids.

experimental conditions reported in the study, the chalcone analogs separated out from the reaction mixture in a matter of minutes. Their purification required the removal by filtration of a small amount of insoluble material prior to their recrystallization. Several of these chalcone analogs have been employed as intermediates in previous literature reports (El-Sabbagh et al. 2009, Li et al. 2012, 2015), but so far only compound **5** has been fully characterized from a structural point of view (Nicholson et al. 2021, Tamuli et al. 2020). The typical characteristic of the proton NMR spectra of these chalcone analogs is the presence of the two doublets having at coupling constant of approximately 15–16 Hz that were assigned to the *trans* protons at the carbon atoms of the double bond in the propenone linker between the two aromatic moieties. One of the doublets associated with these protons is located at approximately 7.3 ppm, and is usually difficult to discriminate owing to its superimposition with signals of other aromatic protons, while the other doublet can be normally identified at approximately 7.8 ppm (Figures S2, S4 and S6). Also, the carbon atoms of

the double bond in the propenone segment of the molecules of chalcone analogs have been usually associated with the two peaks in the 110–120 ppm range in the ^{13}C NMR of these compounds, the peak for the carbon atom in the carbonyl group appears between 188 ppm and 190 ppm, while the rest of the carbon atoms give signals in the expected regions (either aliphatic or aromatic) of the spectra (Figures S3, S5 and S7). Although the aromatic region of the ^{1}H NMR spectra of these chalcones analogs is quite crowded, all the peaks have been fully assigned using 2D NMR experiments, and these assignments for both proton and carbon NMR spectra of chalcone analogs **5**–**7** is given in Experimental.

In the second step of the reaction sequence leading to the target compounds, chalcone analogs **5**–**7** were reacted with excess amount of hydrazine hydrate in 2-propanol at reflux temperature (Figure 1), according to a synthetic procedure previously reported for this type of compounds (Li et al. 2012). The characteristic feature of the pyrazolines unsubstituted at N^1 is their lack of stability over time, which presumably constitutes the main reason for the absence of structural characterization for compounds **8** and **9** in the studies where they were mentioned as intermediates in the preparation of more stable derivatives (Li et al. 2012, 2015). The stability of N^1-unsubstituted pyrazolines investigated in this study seemed to depend on the nature of the moiety at position 3 of the pyrazoline ring and also on the post-synthetic treatments of these compounds. Thus, while pyrazolines **8** and **9** could be kept on the bench after their filtration from the reaction mixture and subsequent washing with a mixture of 2-propanol–hexanes for several days without any visible changes, colorless crystalline pyrazoline derived from chalcone analog **7** turned into a brown semi-solid after one day under the same conditions. In addition, pyrazoline **8**, which was recovered as colorless crystals after recrystallization from 96% ethanol, gradually developed a yellow hue over time. An attempt to recrystallize pyrazoline **9** from 96% ethanol proved detrimental, as only yellow crystals separated when the initial colorless solution became yellow upon cooling. A marked instability was also noticed in the case of samples of N^1-unsubstituted pyrazolines during NMR analysis. When the colorless crystals of pyrazoline **8** were dissolved in $CDCl_3$ that had been kept over anhydrous K_2CO_3, the sample developed immediately a slight yellow color, and the proton NMR spectrum of this sample presented, besides the usual signals of pyrazoline, other low-intensity signals that could not be attributed to the proposed structure. Over time, the color of the NMR sample became more intense, while the intensity of the unknown signals also grew when the proton NMR spectrum was recorded again after 30 minutes, while the peaks assigned to pyrazoline **8** disappeared almost completely after 24 hours (Figure S8). Pyrazoline **8** appeared to be more stable in DMSO-d_6, as a sample from the same colorless batch provided a proton NMR spectrum that was in agreement with the proposed structure and was also free of unknown signals when the experiment was performed straightway. However, a series of new signals could be evidenced even in the proton NMR spectrum of pyrazoline **8** taken in DMSO-d_6 when the experiment was repeated after 20 hours. Therefore, all characterization of N^1-unsubstituted pyrazolines **8** and **9** described in this study consists of data gathered in a timely fashion for materials obtained after the work-up procedure detailed in Experimental, which were deemed sufficiently pure by NMR. Given its lack of stability, no attempt was made to further use the pyrazoline derived from chalcone analog **7** in the synthesis of the target structures.

The ^{1}H NMR spectra of compounds **8** and **9** that were recorded in DMSO-d_6 show the

characteristic signals for the pyrazoline ring, which are the three groups of signals for the mutually coupled, magnetically non-equivalent protons C3-H_X, C2-H_A and C2-H_M that form an AMX three-spin system (Badavath et al. 2016, Matiadis et al. 2020) shown in Figure S9 in Supplementary Material. The peak for the proton of the nitrogen atom (NH) appears in the spectrum of pyrazoline **8** at 7.52 ppm as a doublet owing to its coupling with the proton at the neighboring carbon atom (C3-H_X) at position 5 of the pyrazoline ring (Figure S10), while the doublet of the same proton in the structure of pyrazoline **9** appears at 7.62 ppm, but is less noticeable because of its overlapping with the signal associated with two protons from the chlorine-substituted phenyl ring (Figure S12). The coupling between the signals for NH and C3-H_X was also noticeable in the H,H-COSY spectra of these two compounds. The peak for C3-H_X is observed at 4.79–4.81 ppm as a triplet of doublets with J_{AX} = J_{MX} = 10.6–10.7 Hz and $J_{NH\text{-}Hx}$ = 2.5–2.9 Hz, due to its coupling with NH and with the two magnetically non-equivalent protons (C2-H_A and C2-H_M) of the pyrazoline methylene group. Proton H_A appears at 2.82 ppm as a doublet of doublets with J_{AM} = 16.2–16.3 Hz and J_{AX} = 10.6–10.7 Hz. Proton H_M also appears as a doublet of doublets at about 3.40 ppm with J_{AM} = 16.2–16.3 Hz and J_{MX} = 10.6–10.7 Hz. As the coupling constants of H_X with either H_A or H_M are identical, it is not possible to assign a *cis* or *trans* configuration for the protons at C2 beyond any doubt. All the signals for the aromatic protons in the substituents of these pyrazolines are accounted for and have been assigned an exact and correct chemical shift value. The ^{13}C NMR spectra of pyrazoline **8** and **9** are also in agreement with the proposed structures (Figures S11 and S13). The peak for the carbon atom involved in the double bond with the nitrogen appears at about 147 ppm, the carbon atom in the pyrazoline methylene group gives a peak at approximately 40 ppm, while the peak for the carbon atom in CH appears at about 63 ppm. Discrimination in the ^{13}C NMR spectra of pyrazoline **8** and **9** between the pair C13 and C15 and the pair C19 and C21 was not possible beyond any doubt because of the overlapping of the correlation peaks in the H,C-HSQC and H,C-HMBC spectra of these compounds. Assignment of the signals in the ^{1}H and ^{13}C NMR spectra of pyrazolines **8** and **9** has been accomplished using 2D NMR experiments, and is given in Experimental.

Acylation, sulfonylation, addition to isothiocyanates, alkylation, aminoalkylation and nitrosation are representative amongst the types of reactions that have been so far reported in the literature for the functionalization at position 1 of *N*^{1}-unsubstituted pyrazolines. A synthetic plan was devised to introduce a linker between the benzaldehyde moiety and the pyrazoline scaffold that would enable a facile connection of the two fragments that are required in the structure of the target compounds. In order to allow the stepwise, controlled construction of the target compounds, the linker should derive from a bifunctional molecule whose reactive groups present distinct reactivities towards *N*^{1}-unsubstituted pyrazolines. Such a bifunctional molecule may belong to the class of haloalkyl halides in general (and to halides of haloacetic acids in particular), whose acylation of pyrazolines is a well-established and thoroughly investigated type of reaction. Consequently, *N*^{1}-unsubstituted pyrazolines **8** and **9** were reacted with bromoacetyl bromide in the next step of the reaction sequence leading to the target benzaldehyde–pyrazoline hybrids (Figure 1). An attempt to conduct the reaction of compound **8** with bromoacetyl bromide in the presence of triethylamine in toluene led to a crude material from which the isolation of the desired compound was challenging and afforded only low yields. On the other hand, when the condensation of pyrazolines **8** and **9** with bromoacetyl bromide

was conducted in chloroform in the presence of anhydrous K_2CO_3, access to pure bromoacetyl-substituted pyrazolines **10** and **11** in good yields was achieved through simple recrystallization. Upon inspection of the ^{1}H NMR spectra of intermediates **10** and **11**, the peak for NH could no longer be found, which is indicative for the *N*-acylation of the starting *N*^{1}-unsubstituted pyrazolines (Figures S14 and S16). The protons in the pyrazoline ring give three sets of doublets of doublets: for C2-H_A at approximately 3.20 ppm, for C2-H_M at approximately 4.30 ppm, and for C3-H_X at 5.55 ppm. For these two pyrazolines, the value of the coupling constant between H_M and H_X (J_{MX} = 11.7 Hz) is greater than the value of the coupling constant between H_A and H_X (J_{AX} = 4.4 Hz), which suggest that H_M and H_X are on the same side of the pyrazoline ring (*cis* configuration), while H_A and H_X are on opposite sides of the pyrazoline ring (*trans* configuration) (Muzalevskiy et al. 2021, Zampieri et al. 2008). In addition, because of the structural rigidity of the molecule, the two protons of the bromoacetyl group give two doublets at approximately 4.3 ppm with a geminal coupling constant of 10.4 Hz, that is typical for an AB spin system. All the signals for the protons in the aromatic substituents of pyrazolines **10** and **11** are accounted for, and have been assigned an exact and correct chemical shift value using correlation experiments. The ^{13}C NMR spectra of intermediates **10** and **11** also support the proposed structures, as they exhibit the peaks for the bromoacetyl moiety at about 27 ppm for the carbon atom of the methylene group and at 164 ppm for the carbon atom of the carbonyl function (Figures S15 and S17). Again, the peak for the pair C13 and C15 could not be distinguished from the peak for the pair C19 and C21 because of the overlapping of the correlation peaks in the H,C-HSQC and H,C-HMBC spectra of these compounds. The assignment of the signals in the proton and carbon NMR spectra of intermediates **10** and **11** has been made using 2D NMR experiments, and is provided in Experimental.

Finally, the benzaldehyde moiety was grafted onto the bromoacetyl-substituted pyrazoline scaffold in the last step of the reaction sequence leading to the target compounds **12** and **13** through the substitution of the halogen by a 4-hydroxybenzaldehyde moiety (Figure 1). Surprisingly, this synthetic approach towards aryloxyacetyl-substituted pyrazolines has been reported only recently for the preparation of two series of compounds with anticancer activity (Kumar et al. 2021, Ramaa et al. 2021). We decided to explore a different set of reaction conditions for the synthesis of target benzaldehyde-pyrazoline hybrids **12** and **13** than those previously reported in literature (stirring in *N*,*N*-dimethylformamide at room temperature in the presence of anhydrous K_2CO_3 for 24 h) for structurally related compounds. Thus, heating a mixture of intermediate pyrazolines **10** and **11**, 4-hydroxybenzaldehyde and KOH in 96% ethanol at reflux temperature for 1 h afforded with high yields crude materials that could be considered pure for most synthetic purposes; their recrystallization proceeded with significant weight loss, and resulted in a recovery in moderate yields of compounds **12** and **13** that were deemed sufficiently pure for spectroscopic investigations.

The assignment of the bands for C=O stretching vibration corresponding to the carbonyl in the formyl group and also to the carbonyl in the acetyl function in the IR spectra of target compounds **12** and **13** proved to be slightly challenging, as both bands are partially superimposed (Figures S18 and S21). In the case of pyrazoline **12**, one of these C=O stretching vibration bands appears as a barely noticeable shoulder to the other more intense band at 1687 cm^{-1}, but a noticeable gap between the C=O stretching vibration bands at 1693 cm^{-1} and 1683 cm^{-1} in the spectra of pyrazoline **13** allows for

their facile discrimination. Other characteristic absorption band in the IR spectra of compounds **12** and **13** is the strong peak at 1601 cm^{-1} and 1599 cm^{-1}, respectively, which was assigned to the stretching vibration of the C=N in the pyrazoline ring (Laude & Khanh 1975).

A comparison between the proton NMR spectra of these target compounds and those of their corresponding parent compounds **10** and **11** indicated that the one of the most noticeable differences is a consequence of the substitution of bromine with the aryloxy moiety, which results in an increase of the chemical shift value of the two doublets associated with the protons in the acetyl fragment with almost 1 ppm, from 4.3 ppm to approximately 5.3 ppm (Figures S19 and S22). The presence in the spectra of benzaldehyde–pyrazoline hybrids **12** and **13** of a singlet at 9.87 ppm that was assigned to the formyl group proton also supports the replacement of the bromine in intermediates **10** and **11** with the aryloxy moiety. The magnetically non-equivalent protons in the pyrazoline ring give three sets of doublets of doublets for C2-H_A at 3.22–3.26 ppm, for C2-H_M at 3.75–3.78 ppm and for C3-H_X at 5.58 ppm. Like in the case of intermediates **10** and **11**, the values of the coupling constants between H_X and H_M and H_A suggest that the conformation of H_X and H_A is *trans*, while the conformation of H_X and H_M is *cis*. The signals from the large number of protons in the aromatic rings generally overlap in non-distinctive multiplets in the crowded region between 6.9 ppm and 7.8 ppm, but their number is in agreement with the number of the protons in the proposed structure, and the assignment of particular signals to a specific type of proton in the structure of compounds **12** and **13** was accomplished using correlation experiments. In the ^{13}C NMR spectra of benzaldehyde–pyrazoline hybrids **12** and **13**, the peak at approximately 190 ppm is indicative for the carbon atom in the formyl group, while the shift of the peak at about 27 ppm (that was attributed to the carbon atom in the methylene group from the acetyl fragment in intermediates **10** and **11**) to approximately 66 ppm for the same carbon atoms in target compounds **12** and **13** is also suggestive for the substitution of bromine with the aryloxy moiety (Figures S20 and S23). All the other peaks in the ^{1}H and ^{13}C NMR spectra of benzaldehyde–pyrazoline hybrids **12** and **13** have been fully assigned using 2D NMR experiments, and are detailed in Experimental.

The photophysical properties of pyrazolines depend strongly on the intramolecular charge transfer processes that could take place, which are influenced by the nature of substituents at N1, C3 and C5 in the pyrazoline ring (Varghese et al 2017). The presence of an electron-donating moiety at N1 that is coupled with an electron-accepting moiety at C3 enables a dominant charge transfer through the extended conjugated system formed by the linker containing atoms N1, N2 and C3 within the pyrazoline ring, and the corresponding electronic transitions that take place are similar to π–π* electronic transitions. In this scenario, the N1-N2-C3 linker together with the substituents at N1 and C3 represents the main chromophore in pyrazolines, although a secondary intramolecular charge transfer involving the non-conjugated system formed by N1-C5 and these atoms' substituents is possible. Nonetheless, an intramolecular charge transfer through the latter system is usually minor, less likely to occur, and is also strongly affected by the local conformation of the molecule (Varghese et al 2017). Because the target compounds **12** and **13** are close structural analogs, their UV spectra are quite similar and present a sole absorption maximum at 292 nm (Figure 2). A shoulder at 320 nm is barely noticeable in the UV spectrum of pyrazoline **13**, which suggests the existence of some specific electronic transitions that are induced by the participation of the chlorine substituent in the phenyl ring at C3 of the pyrazoline ring to

the conjugated system N1-N2-C3. On the other hand, the hypsochromic shift of the absorption maximum for benzaldehyde–pyrazoline hybrids **12** and **13** from values above 350 nm (that are normal for 1,3,5-triarylpyrazolines (Chibac et al. 2019a, Bozkurt & Gul 2018, Hasan et al. 2011)) to values below 300 nm is a direct consequence of the lack of substituent at N1 that could contribute to the extension of the conjugated system N1-N2-C3. Therefore, the electronic transitions take place in the case of pyrazolines **12** and **13** within a conjugated system that is less extended that the conjugated system of 1,3,5-triarylpyrazolines. The fluorescence spectra of the target compounds **12** and **13**, for which the maximum of emission was obtained for an excitation wavelength of 292 nm, also share a similar profile (Figure 3). However, a couple of characteristics set these two emission spectra apart. First, the emission maxima for the two structurally analogous compounds are slightly different, as the emission maximum for compound **12** is at 340 nm, while the emission maximum for compound **13** is at 360 nm. Second, the fluorescence intensity for pyrazoline **13** is almost twice as high as the fluorescence intensity of pyrazoline **12**. Because the benzaldehyde–pyrazoline hybrids **12** and **13** are very much alike, the dissimilarities observed in their optical behavior are presumably associated with the replacement of the hydrogen atom in the phenyl substituent at C3 in the pyrazoline ring with a chlorine atom. The introduction of a *para*-substituent with an electron-withdrawing effect in the electron-accepting phenyl moiety at C3 of pyrazoline **13** clearly increases the degree of electron delocalization within this compound compared to its unsubstituted analog **12**, and ultimately produces an amplification of the intramolecular charge transfer. This postulation is in line with the conclusions of a study concerning the effect of electron-accepting and electron-withdrawing substituents of the phenyl moieties at N1 and C3 on the photophysical properties in a series of 1,3,5-triarylpyrazolines (Fahrni et al. 2003), and supports the hypothesis that the introduction of other substituents with a more pronounced electron-withdrawing effect (*e.g.*, cyano or carbalkoxy) on the phenyl moiety at C3 in the pyrazoline scaffold that compounds **12** and **13** share would further augment the fluorescence intensity of the resulting analogs.

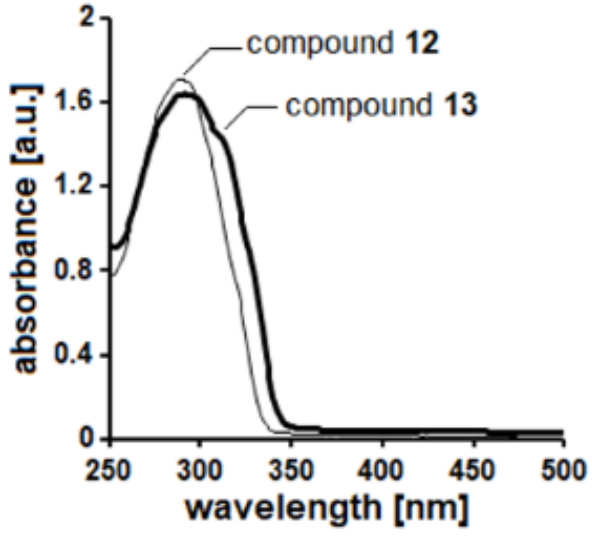

Figure 2. UV–vis spectra of compounds 12 and 13.

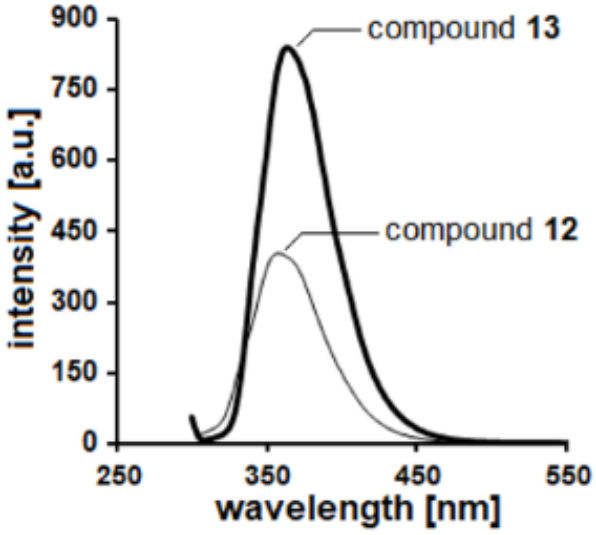

Figure 3. Fluorescence spectra of compounds 12 and 13.

REFERENCES

ANTONY R, ARUN T & MANICKAM STD. 2019. A review on applications of chitosan-based Schiff bases. Int J Biol Macromol 129: 615-633.

BADAVATH VN, BAYSAL İ, UCAR G, SINHA BN & JAYAPRAKASH V. 2016. Monoamine oxidase inhibitory activity of novel pyrazoline analogues: Curcumin based design and synthesis. ACS Med Chem Lett 7: 56-61.

BALE AT ET AL. 2018. Chalcones and bis-chalcones: As potential α-amylase inhibitors; synthesis, *in vitro* screening, and molecular modelling studies. Bioorg Chem 79: 179-189.

BOZKURT E & GUL HI. 2018. A novel pyrazoline-based fluorometric "turn-off" sensing for Hg^{2+}. Sens Actuators B 255: 814-825.

CHEN Z, LV Z, SUN Y, CHI Z & QING G. 2020. Recent advancements in polyethyleneimine-based materials and their biomedical, biotechnology, and biomaterial applications. J Mater Chem B 8: 2951-2973.

CHIBAC AL, ROMAN G, COJOCARU C, SĂCĂRESCU G, SIMIONESCU M & SĂCĂRESCU L. 2019b. Pyrazoline based chloride sensor for body fluids screening. J Mol Liq 284: 139-146.

CHIBAC AL, ROMAN G, COJOCARU C, SHOVA S, SĂCĂRESCU G, SIMIONESCU M & SĂCĂRESCU L. 2019a. Bichromophoric pyrazoline derivative with solvent-selective photoluminescence quenching. J Mol Liq 278: 156-163.

CHIBAC-SCUTARU AL, COJOCARU C, COROABĂ A, ROMAN G, SĂCĂRESCU G, SIMIONESCU M & SĂCĂRESCU L. 2020. Nano-assembled oligosilane-pyrazoline structures and their optical properties. J Mol Liq 303: 112657.

EL-SABBAGH OI, BARAKA MM, IBRAHIM SM, PANNECOUQUE C, ANDREI G, SNOECK R, BALZARINI J & RASHAD AA. 2009. Synthesis and antiviral activity of new pyrazole and thiazole derivatives. Eur J Med Chem 44: 3746-3753.

FAHRNI, CJ, YANG, L & VANDERVEER, DG. 2003. Tuning the photoinduced electron-transfer thermodynamics in 1,3,5-triaryl-2-pyrazoline fluorophores: X-ray structures, photophysical characterization, computational analysis, and in vivo evaluation. J Am Chem Soc 125: 3799-3812.

FAROOQ S & NGAINI Z. 2019. One-pot and two-pot synthesis of chalcone based mono and bis-pyrazolines. Tetrahedron Lett 61: 151416.

HASAN A, ABBAS A & AKHTAR MN. 2011. Synthesis, characterization and fluorescent property evaluation of 1,3,5-triaryl-2-pyrazolines. Molecules 16: 7789-7802.

HEINZE T, SIEBERT M, BERLIN P & KOSCHELLA A. 2016. Biofunctional materials based on amino cellulose derivatives - a nanobiotechnological concept. Macromol Biosci 16: 10-42.

IFTIKHAR S, KHAN S, BILAL A, MANZOOR S, ABDULLAH M, EMWAS A-H, SIOUD S, GAO X, CHOTANA GA, FAISAL A & SALEEM RSZ. 2017. Synthesis and evaluation of modified chalcone based p53 stabilizing agents. Bioorg Med Chem Lett 27: 4101-4106.

KUMAR AP, MEYER-ALMES FJ, RAMAA CS, SAFUAN S, SCHWEIPERT M, TILEKAR K & UPADHYAY N. 2021. Double-edged swords: Diaryl pyrazoline thiazolidinediones synchronously targeting cancer epigenetics and angiogenesis. Bioorg Chem 116: 105350.

LAUDE B & KHANH LQ. 1975. Etude spectroscopique (u.v., i.r. et NMR) de diphényl-1,3 aryl-5 pyrazolines-2. Influence de la substitution du noyau aromatique en 5. Spectrochim Acta Part A 31: 1121-1126.

LÉVAI A. 2002. Synthesis of 2-pyrazolines by the reactions of α,β-unsaturated aldehydes, ketones, and esters with diazoalkanes, nitrile imines, and hydrazines. J Heterocycl Chem 39: 1-13.

LI C, LI Q, YAN L, SUN X, WEI R, GONG H & ZHU H. 2012. Synthesis, biological evaluation and 3D-QSAR studies of novel 4,5-dihydro-1*H*-pyrazole niacinamide derivatives as BRAF inhibitors. Bioorg Med Chem 20: 3746-3755.

LI Q, LII X, YANG Y, RUAN B, YAO R & LIAO C. 2015. Discovery and pharmacophore studies of novel pyrazole-based anti-melanoma agents. Chem Biodiversity 12: 116-132.

LIAO L, DENG B & LEI G. 2017. Preparation and properties of novel polymer blue fluorescent materials. Spectrosc Spectral Anal (Beijing, China) 37: 636-640.

ŁUBKOWSKA M & STAŃCZYK W. 2014. Aminoalkyl functionalized siloxanes. Polimery (Warsaw) 59: 683-686.

MAHESHA P, SHETTY NS, & KULKARNI SD. 2022. A review on metal ion sensors derived from chalcone precursor. J Fluoresc 32: 835-862.

MANGALA K & SREEKUMAR K. 2015. Dendrimer functionalized polysilane: an efficient and recyclable organocatalyst. J Appl Polym Sci 132: 41593.

MATIADIS D, MAVROIDI B, PANAGIOTOPOULOU A, METHENITIS C, PELECANOU M & SAGNOU M. 2020. (*E*)-(1-(4-Ethoxycarbonylphenyl)-5-(3,4-dimethoxyphenyl)-3-(3,4-dimethoxystyryl)-2-pyrazoline: Synthesis, characterization, DNA-interaction, and evaluation of activity against drug-resistant cell lines. Molbank 2020: M1114.

MUZALEVSKIY VM, SIZOVA ZA, PANYUSHKIN VV, CHERTKOV VA, KHRUSTALEV VN & NENAJDENKO VG. 2021. α,β-Disubstituted CF_3-enones as a trifluoromethyl building block:

Regioselective preparation of totally substituted 3-CF_3-pyrazoles. J Org Chem 86: 2385-2405.

NICHOLSON K, LANGER T & THOMAS SP. 2021. Borane-catalyzed, chemoselective reduction and hydrofunctionalization of enones enabled by B-O transborylation. Org Lett 23: 2498-2504.

RAMAA CS, KUMAR AP, MEYER-ALMES FJ, SAFUAN S, SCHWEIPERT M, TILEKAR K & UPADHYAY N. 2021. Multi-target weapons: diaryl-pyrazoline thiazolidinediones simultaneously targeting VEGFR-2 and HDAC cancer hallmarks. RSC Med Chem 12: 1540-1554.

SĂCĂRESCU L, CHIBAC-SCUTARU AL, ROMAN G, SĂCĂRESCU G & SIMIONESCU M. 2023. Selective detection of metal ions, sulfites and glutathione with fluorescent pyrazolines: a review. Environ Chem Lett 21: 561-596.

SZUKALSKI A, HAUPA K, MINIEWICZ A & MYSLIWIEC J. 2015. Photoinduced birefringence in PMMA polymer doped with photoisomerizable pyrazoline derivative. J Phys Chem C 119: 10007-10014.

TAMULI KJ, SAHOO RK & BORDOLOI M. 2020. Biocatalytic green alternative to existing hazardous reaction media: Synthesis of chalcone and flavone derivatives via the Claisen-Schmidt reaction at room temperature. New J Chem 44: 20956-20965.

VAHEDPOUR T, HAMZEH-MIVEHROUD M, HEMMATI S & DASTMALCHI S. 2021. Synthesis of 2-pyrazolines from hydrazines: mechanisms explained. ChemistrySelect 6: 6483-6506.

VARGHESE B, AL-BUSAFI SN, SULIMAN FO & AL-KINDY SMZ. 2017. Unveiling a versatile heterocycle: Pyrazoline - a review. RSC Adv 7: 46999-47016.

ZAMPIERI D, MAMOLO MG, LAURINI E, SCIALINO G, BANFI E & VIO L. 2008. Antifungal and antimycobacterial activity of 1-(3,5-diaryl-4,5-dihydro-1*H*-pyrazol-4-yl)-1*H*-imidazole derivatives. Bioorg Med Chem 16: 4516-4522.

ZERAFA N, CINI M & MAGRI DC. 2021. Molecular engineering of 1,3,5-triaryl-2-pyrazoline fluorescent logic systems responsive to acidity and oxidisability and attachment to polymer beads. Mol Syst Des Eng 6: 93-99.

SUPPLEMENTARY MATERIAL

Figures S1-S23.

How to cite

ROMAN G, BALAN-PORCĂRAŞU M & SĂCĂRESCU L. 2024. Development of benzaldehyde-pyrazoline hybrids for functionalization of polymers with fluorescent pendant moieties. An Acad Bras Cienc 96: e20220875. DOI 10.1590/0001-3765202420220875.

Manuscript received on October 7, 2022;
accepted for publication on April 16, 2023

GHEORGHE ROMAN[1]
https://orcid.org/0000-0003-0939-1899

MIHAELA BALAN-PORCĂRAŞU[2]
https://orcid.org/0000-0001-8988-070X

LIVIU SĂCĂRESCU[1]
https://orcid.org/0000-0002-6543-0277

[1]Petru Poni Institute of Macromolecular Chemistry
Department of Inorganic Polymers, 41A Aleea
Grigore Ghica Vodă, 700487 Iaşi, Romania

[2]Petru Poni Institute of Macromolecular Chemistry,
Department of Polycondensation and Thermostable
Polymers, 41A Aleea Gr. Ghica Vodă, 700487 Iaşi, Romania

Correspondence to: **Gheorghe Roman**
E-mail: gheorghe.roman@icmpp.ro

Author contributions

G. Roman was responsible for conceptualization, investigation, formal analysis, data curation, writing – original draft, writing – review and editing. M. Balan-Porcăraşu contributed to investigation, formal analysis, data curation and writing – original draft. L. Săcărescu is credited for investigation, formal analysis, data curation and writing – original draft.

CC BY